Journal for ImmunoTherapy of Cancer

Triple-serotype chimeric oncolytic adenovirus exerts multiple synergistic mechanisms against solid tumors

Yinghan Su,[1,2] Jiang Li,[2,3] Weidan Ji,[2,3] Gang Wang,[4] Lin Fang,[4] Qin Zhang,[3] Lin Ang,[5] Min Zhao,[5] Yuan Sen,[4] Lei Chen,[2,3] Junnian Zheng,[4] Changqing Su ,[2,3,4] Lunxiu Qin[1]

To cite: Su Y, Li J, Ji W, *et al*. Triple-serotype chimeric oncolytic adenovirus exerts multiple synergistic mechanisms against solid tumors. *Journal for ImmunoTherapy of Cancer* 2022;**10**:e004691. doi:10.1136/jitc-2022-004691

► Additional supplemental material is published online only. To view, please visit the journal online (http://dx.doi.org/10.1136/jitc-2022-004691).

YS and JL contributed equally.

Accepted 02 May 2022

Check for updates

© Author(s) (or their employer(s)) 2022. Re-use permitted under CC BY-NC. No commercial re-use. See rights and permissions. Published by BMJ.

For numbered affiliations see end of article.

Correspondence to
Dr Changqing Su;
suchangqing@gmail.com

Lunxiu Qin; qinlx@fudan.edu.cn

ABSTRACT

Background Oncolytic virotherapy has become an important branch of cancer immunotherapy. This study investigated the efficacy of an oncolytic adenovirus (OAV), OncoViron, with synergistic mechanisms in the treatment of multiple solid tumors.

Methods An OAV, OncoViron, was constructed and investigated by cytological experiments and implanted tumor models of multiple solid tumor cell lines to certify its anticancer efficacy, the synergistic effects of viral oncolysis and transgene anticancer activity of OncoViron, as well as oncolytic virotherapy combined with immunotherapy, were also verified.

Results The selective replication of OncoViron mediated high expression of anticancer factors, specifically targeted a variety of solid tumors and significantly inhibited cancer cell proliferation. On a variety of implanted solid tumor models in immunodeficient mice, immunocompetent mice, and humanized mice, OncoViron showed great anticancer effects on its own and in combination with programmed death 1 (PD-1) antibody and chimeric antigen receptor (CAR) T cells. Pathological examination, single-cell sequencing, and spatial transcriptome analysis of animal implanted tumor specimens confirmed that OncoViron significantly altered the gene expression profile of infected cancer cells, not only recruiting a large number of lymphocytes, natural killer cells, and mononuclear macrophages into tumor microenvironment (TME) and activated immune cells, especially T cells but also inducing M1 polarization of macrophages and promoting the release of more immune cytokines, thereby remodeling the TME for coordinating PD-1 antibody or CAR T therapy.

Conclusions The chimeric OncoViron is a novel broad-spectrum anticancer product with multiple mechanisms of synergistic and potentiated immunotherapy, creating a good opportunity for combined immunotherapy against solid tumors.

BACKGROUND

Gene therapy-mediated by oncolytic virus (OV) is an important and emerging therapeutic strategy for cancer.[1] After Rigvir was approved in Latvia in 2004,[2] Oncorine (H101) in China in 2005,[3] the new milestone for oncolytic virotherapy is the Food and Drug Administration approval of T-VEC (talimogene laherparepvec) in 2015. T-VEC is an oncolytic herpes simplex virus (HSV) and expresses granulocyte–macrophage colony-stimulating factor.[4] Whereafter, oncolytic HSV, Delytact (teserpaturev/G47Δ), was approved in June 2021 in Japan. This is the fourth OV approved worldwide.[5] In addition to the approved OVs, there are currently several OV products that have been tested in phases I–III clinical trials worldwide, from various types of adenoviruses, HSV, coxsackievirus, poxvirus, and reovirus. It has been demonstrated that the cancer cells infected by OVs secrete a large number of cytokines, while the lysed tumor cells release a variety of tumor-associated antigens. Thus, oncolytic virotherapy not only can trigger immune responses but also can alter tumor microenvironment (TME), which enhances the outcome of chemotherapy and radiotherapy and improves the curative effect of immune checkpoint blockade and adoptive cell immunotherapy.[6] In a phase Ib clinical trial of 21 patients with melanoma, the efficacy of T-VEC combined with programmed death 1 (PD-1) antibody was 62%, while that of T-VEC was 40% and that of PD-1 antibody alone was 35%, suggesting that OVs can effectively improve the efficacy of immunotherapy.[7]

The biggest challenge of oncolytic virotherapy is how to improve the safety and efficacy of OV products. In contrast to the natural viral strains that can replicate preferentially in cancer cells and the viral strains that are simply genetically modified to have a certain level of cancer-selective killing specificity, the mechanisms by which adenovirus can be genetically engineered to target cancer cells for replication and killing are greatly varied. For example, the first-generation oncolytic adenoviruses (OAVs) had replication capacity specifically in P53-deficient cancer cells by deleting the

E1b-55kD gene.[3 8] The following second-generation of OAVs employed various cancer-specific promoters to regulate the expression of the adenovirus genes E1a or/and E1b.[9 10] In the third-generation of OAVs, the combination of multiple regulatory elements was developed.[11 12] After several generations and diverse modifications, the increase in the specificity and efficacy of OAVs against various cancers is the most remarkable among all OVs. Theoretically, OAVs as vectors carrying anticancer genes can initiate viral replication strictly within cancer cells, followed by high copy amplification and efficient expression of anticancer genes, resulting in a dual cancer-killing effect of oncolysis by viral replication and tumor suppression by gene expression, without affecting normal cells. However, the cancer-targeting specificity and cancer-killing effect of OVs, including OAV, have not yet met the expectation in practice, and the clinical outcome of OVs alone in treatments remains unsatisfactory.

OncoViron is a chimeric OAV with multiple mechanisms of synergistic anticancer activity, featuring triple regulation for targeting cancer mechanisms, triple modification of viral structural protein genes, triple chimerization within three serotype adenoviruses, and triple transgene by loading three anticancer genes. The advantages of OncoViron lie in the following: (1) the precise regulation of viral replication targeting cancer cells is implemented at both the transcriptional and translational levels; (2) the intrinsic anticancer activity of several viral structural proteins is activated; (3) the ability to infect cancer cells is increased, and the virus itself avoiding the interception from pre-existing neutralizing antibodies and the adsorption by hepatocytes is assured; and (4) three types of anticancer immunomodulatory genes were armed to enhance the effect of killing cancer cells. OncoViron is, therefore, a fourth-generation of the OAV product, which can be used as a stand-alone treatment for a variety of human solid tumors, as well as the most powerful synergist for cancer immunotherapy or other treatments.

MATERIALS AND METHODS

Construction and amplification of viruses

The survivin promoter (−938 bp to +50 bp) was synthesized by referring to the 5′-UTR (untranslated region) of survivin gene (GenBank: U75285) and cloned into the upstream of Ad5 E1a. The 12 bp of the CR2 region (cacgaggctggc) was deleted from E1a to form mutant E1a (mE1a), and the oxygen-dependent degradation (ODD) domain sequence of HIF-1α was fused downstream of mE1a as a genetic on/off switch. Meanwhile, the coding sequences of E1b-55kD and E1b-19kD proteins in the Ad5 E1 region were deleted. The fiber knob sequence of Ad5 was replaced by the corresponding fragment of Ad11, and the hypervariable region (HVR) of Ad5 hexon was selectively substituted with the corresponding sequence of rare serotype Ad48. The E3 region was deleted, but the adenovirus death protein (ADP) was retained, and the expression cassette of two immunomodulatory cytokines [interleukin 12 (IL-12) gene and interferon-γ (IFN-γ) gene] and one chemokine [chemokine RANTES (CCL5) gene] were loaded into the E3 region. The 2A peptide sequence from foot-and-mouth disease virus (F2A) was used to link the transgenes, and a linker (GTTCCTGG AGTAGGGGTACCTGGGGTGGGC) was used to fuse two subunits of IL-12. Finally, a novel OAV, named OncoViron, was generated (figure 1A). We also constructed a series of control viruses (online supplemental figure S1). All the viruses were amplified in HEK293 cells and purified by cesium chloride gradient centrifugation. The viral titer was determined by the 50% tissue culture infective dose method.

Cell lines and cell culture

Twenty-four human cancer cell lines, seven human normal cell lines, and three murine tumor cell lines were mainly purchased from Cell Bank of Shanghai Zhongqiao Xinzhou Biotechnology Co. (China) and China Center (Wuhan) for type culture collection (online supplemental table S1). All cell lines were authenticated and tested by the short tandem repeat method within 6 months prior to use and were cultured according to the instructions provided by the manufacturers. The culture was carried out in a three-gas 37°C incubator containing 5% CO_2, 21% O_2 at normoxic condition, and 5% CO_2, 2% O_2 at hypoxia condition.

Methodology

Detailed methods are provided in the online supplemental materials & methods.

RESULTS

OncoViron is endowed with a high cancer-selective replication activity

In OncoViron genome, the survivin promoter is used to control viral selective replication targeting cancer cells at the transcriptional level, and the ODD element as genetic on/off switch is used to limit viral replication in normal cells at the translational level (figure 1A). When cells were infected with OncoViron under normoxia culture, the virus achieved high copy replication in solid tumor cell lines. At 96 hours after infection, the maximum replication activity was 316 979-fold increased in HCCLM3 and MHCC97H cells of hepatocellular carcinoma, and NOZ and GBC-SD cells of gallbladder cancer, while the replication activity was very low in normal cell lines GES-1, BJ, and L02, the maximum replication activity was only 399-fold increased in L02 cells (figure 1B). The Ad5/Ad11 fiber chimeric virus Ad5SVPF11 and all generated viruses carrying single, double, or triple cytokines could also replicate in various solid tumor cells with high copies. However, their replication activity was low in normal cells (online supplemental figure S2A). It was confirmed that the loading of multiple cytokine genes on Ad5SVPF11 did not affect viral cancer-selective replication activity. The viral replication and mE1a expression of OncoViron

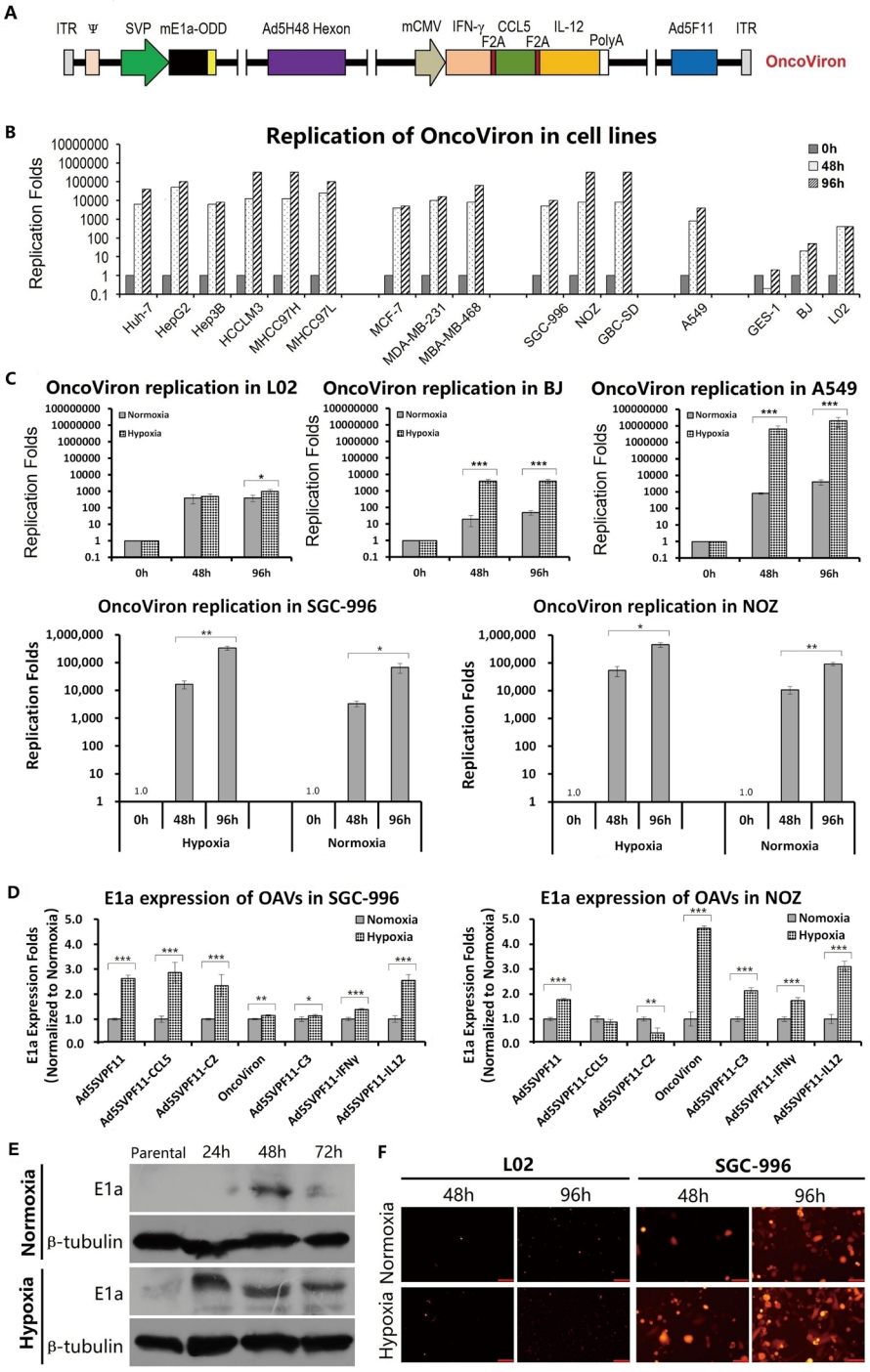

Figure 1 Cancer-selective replication of OncoViron and its control viruses. (A) The structural schematic diagram of OncoViron. (B) The replicative activity of OncoViron in multiple cell lines. Cells were seeded in 96-well plates, 1×10^4/well, and viruses were added at MOI=5 pfu/cell. Cells were collected at 96 hours, and viral titer was detected by TCID50. (C) Comparison of replication ability of OncoViron in cancer and normal cells under hypoxia and normoxia. Cells were cultured under 37℃ saturated humidity and 5% CO_2, 21% O_2 normoxic condition, 5% CO_2, and 2% O_2 hypoxic condition, respectively, and infected with virus at MOI=5 pfu/cell. Viral titer was detected by TCID50 method at 48 and 96 hours after infection. (D) Expression of E1A in OAV-infected cancer cells under hypoxia and normoxia. (E) OncoViron-mediated E1A expression in A549 cells under hypoxia detected by Western blotting. β-tubulin was used as a loading control. Parental: A549 parental cells without infection of virus. (F) comparison of DsRed expression mediated by Ad5SVPF11H48-DsRed in cancer cells and normal cells. bar: 50 µm. *P<0.05, **P<0.01, ***P<0.001. ψ, adenovirus packaging signal; Ad5F11, chimeric fiber coding sequence of Ad5 and Ad11; Ad5H48 hexon, chimeric hexon coding sequence of Ad5 and Ad48; CCL5, chemokine RANTES gene; F2A, 2A peptide sequence from foot-and-mouth disease virus; IFN-γ, interferon-γ; IL-12, interleukin 12; ITR, inverted terminal repeat; mCMV, mouse cytomegalovirus promoter; mE1a-ODD, mutated E1a gene with C-terminal fusion of oxygen-dependent degradation domain; MOI, multiplicity of infection; OAV, oncolytic adenovirus; PolyA, SV40 poly(A) sequence; SVP, survivin promoter; TCID50, 50% tissue culture infective dose.

were consistent with the survivin levels in various cell lines. Even in survivin weakly positive cancer cell lines, the viral replication was higher than that in survivin-positive normal cells (online supplemental figure S2B,C). OncoViron still maintained high cancer-selective replication activity after chimerizing Ad5/Ad48 hexon (online supplemental figure S2D).

To verify the regulation of the ODD switch, cells were cultured under hypoxia condition and the hypoxia significantly promoted OncoViron replication in A549, SGC-996, and NOZ cancer cells. OncoViron replication also increased in normal cells under hypoxia, but not as much as in cancer cells (figure 1C). The mE1a expression was generally upregulated under hypoxia in cancer cells which were infected with OncoViron and its control viruses (figure 1D). OncoViron-mediated mE1a expression in A549 cells under hypoxia increased compared with the normoxic condition (figure 1E), suggesting that ODD played a role in degrading E1a under normoxic condition. The expression of red fluorescent protein (DsRed) was observed under fluorescent microscope at 96 hours after cell infection with the Ad5SVPF11H48-DsRed virus. Under normoxic condition, the Ad5SVPF11H48-DsRed-infected L02 cells continuously expressed low levels of DsRed, whereas DsRed was highly expressed in SGC-996 cells. Under hypoxia, Ad5SVPF11H48-DsRed mediated slightly enhanced DsRed expression in L02 cells but significantly was enhanced in SGC-996 cells (figure 1F).

Chimerization of fiber Ad5F11 and hexon Ad5H48 enhances the infectivity and improves the function of OncoViron

Coxsackievirus–adenovirus receptor (CAR) is the receptor for Ad5. Ad5 fiber was chimerized with Ad11-fiber to form a chimeric fiber Ad5F11 which could also recognize CD46 as its receptor. Flow cytometry (FCM) found that the expression levels of CD46 were higher than CAR in most cancer cell lines (figure 2A), and the infectivity of the Ad5F11-chimeric virus Ad5SVPF11H48-DsRed was significantly stronger than that of the Ad5-fiber virus Ad5SVPH48-EGFP in most cancer cell lines. In cancer cell lines with high expression of both CAR and CD46 (eg, Huh-7 and MDA-MB-231), both Ad5SVPF11H48-DsRed and Ad5SVPH48-EGFP had high infectivity, but Ad5SVPF11H48-DsRed was still stronger than Ad5SVPH48-EGFP. In cancer cell lines with low CAR expression and high CD46 expression (such as MCF-7 and OSRC-2), the infectivity of Ad5SVPF11H48-DsRed was very strong, whereas the infection of Ad5SVPH48-EGFP was very low (figure 2B). The results showed that the chimerization of Ad5F11 significantly enhanced the infectivity of OAV in most cancer cells.

The Ad5-hexon was chimerized with Ad48-hexon to form a chimeric hexon Ad5H48 which could help adenovirus evade interception by pre-existing immune-neutralizing antibodies. BALB/C mice were first injected into the tail vein of wild Ad5 (wAd5) and then injected into the tail vein of OncoViron and Ad5SVPF11-C3 at 48 hours later, respectively; blood, heart, liver, lung, kidney, and brain of mice were collected 96 hours later. Peripheral blood mononuclear cells (PBMCs) were isolated from mouse blood, and the expression of mE1a mRNA in PBMCs was positive in both OncoViron and Ad5SVPF11-C3 groups. After prior immunization with wAd5, the expression of wE1a was positive in the OncoViron+wAd5 and Ad5SVPF11-C3+wAd5 groups. The OncoViron+wAd5 group was also positive for mE1a, but the Ad5SVPF11-C3+wAd5 group was nearly negative for mE1a (figure 2C). By immunohistochemistry, E1a protein was negative in heart, lung, kidney, and brain tissues of mice in all groups but positive in liver tissues in wAd5 preimmunization group and nearly negative in other groups (figure 2D and online supplemental figure S3A). The results showed that chimerization of Ad5H48 endowed OncoViron with an ability to effectively resist interception by neutralizing antibodies produced by wAd5 preconditioning, and hepatocyte adhesion and infection with OncoViron were also significantly reduced.

OncoViron mediates high expression of anticancer cytokines

Cells were infected with OncoViron, and a series of control viruses at a multiplicity of infection (MOI)=5 pfu/cell, the content of IFN-γ, IL-12, and CCL5 in the supernatants of cultured cells, were detected at 24, 48, and 72 hours by ELISA. OncoViron and Ad5SVPF11-C3 were found to mediate high expression of the three cytokines with a time-dependent manner (figure 3A). Ad5SVPF11H48-DsRed replicated and expressed DsRed efficiently in cancer cells, whereas the non-replicating virus Ad5-EGFP mediated a low level of EGFP (figure 3B). Ad5SVPF11-IL12, Ad5SVPF11-CCL5, and Ad5SVPF11-C2 that carried single or double cytokines, respectively, also efficiently expressed high levels of the corresponding cytokines in experimental cell lines (online supplemental figure S3B). Ad5SVPF11H48-mC3 carried three murine cytokine genes, and the transgenes were also highly expressed in virus-infected HEK293 cells (figure 3C).

OncoViron affects the transcriptional expression profile of cancer cells

The effect of OncoViron on cell transcriptional expression profile was analyzed by setting a threshold DESeq2_EBSeq FDR=0.05 FC=2. Six OAVs, including OncoViron, Ad5SVPF11H48, Ad5SVPF11, Ad5SVPF11-IL12, Ad5SVPF11-CCL5, and Ad5SVPF11-IFNγ, all caused changes of mRNA expression profiles in HCCLM3, MDA-MB-231, SGC-996, and MRC-5 cell lines (online supplemental table S2), and OncoViron induced more pronounced changes than the control viruses (figure 3D and online supplemental figure S3C). The differentially expressed genes (DEGs) were mainly enriched in the focal adhesion of cellular process and the function of phagosome, and in PI3K-Akt, cytokine–cytokine receptor interaction, and MAPK pathways (figure 3E). Analysis from the Kyoto Encyclopedia of Genes and Genomes (KEGG) enrichment classification diagram and the network diagram showed that the number of DEGs in

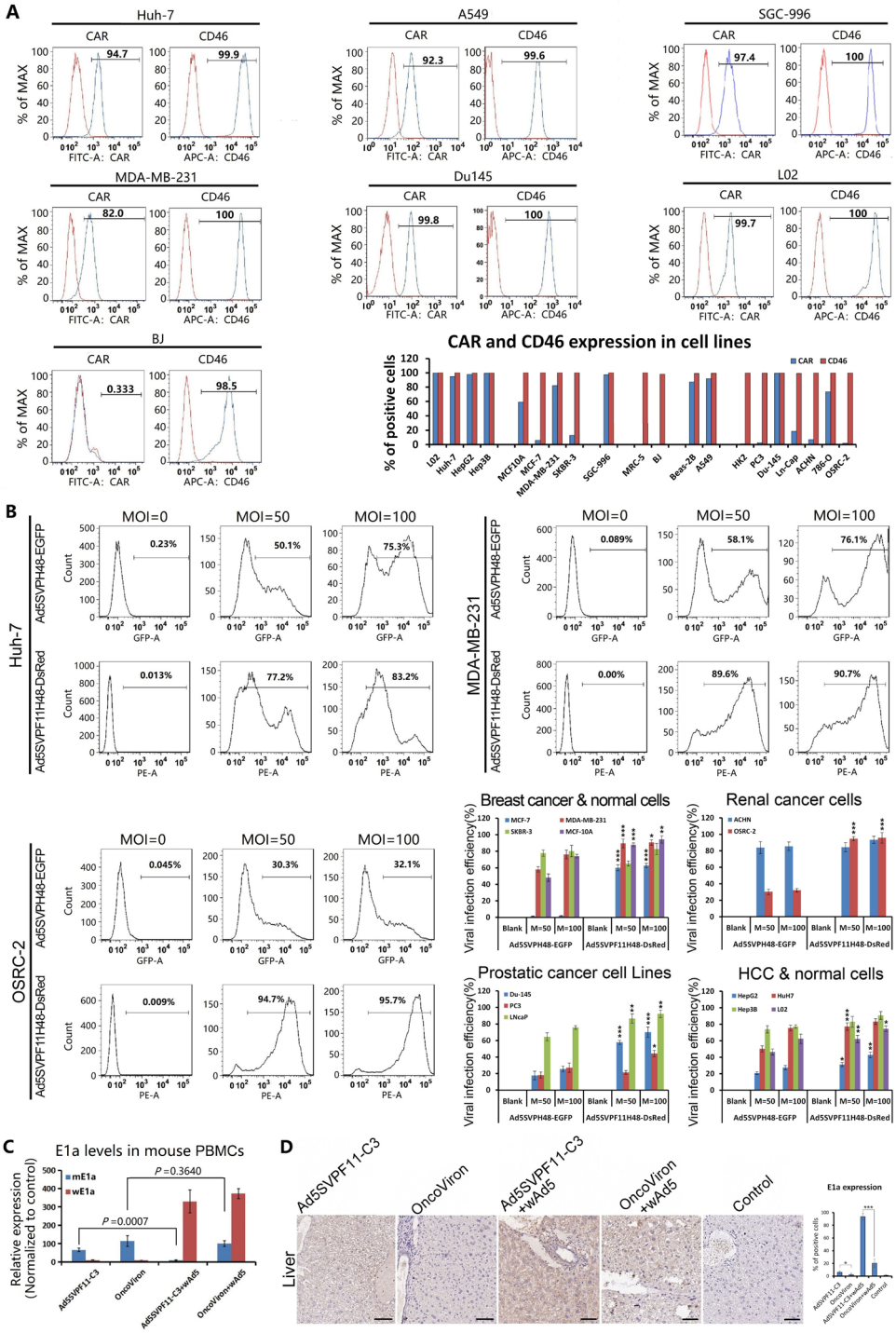

Figure 2 Functional characterization of chimeric fiber Ad5F11 and chimeric Ad5H48 hexon. (A) The expression of CAR and CD46 in experimental cell lines was detected by FCM. (B) The effect of chimeric fiber Ad5F11 on viral infectivity. Cells were seeded in six-well plates, 3×10^5 cells/well, infected with Ad5SVPF11H48-DsRed with Ad5F11-chimerized and Ad5SVPH48-EGFP without Ad5F11-chimerized at MOI=50 and 100 pfu/cell, and collected 24 hours later. The fluorescent intensity was detected by FCM in each cell line. *P<0.05, **P<0.01, ***P<0.001 compared with Ad5SVPH48-EGFP at the same MOI. (C) BALB/c mice were injected with Ad5 by tail vein at 1×10^8 pfu/0.1 mL/mouse, and OncoViron with Ad5H48-chimerized and Ad5SVPF11-C3 without Ad5H48-chimerized at 1×10^9 pfu/0.1 mL/mouse were injected 48 hours later. Blood was collected 96 hours later, and the expression of wE1a and mE1a was detected by qRT-PCR in blood PBMCs. (D) E1A protein was detected by immunohistochemistry in mouse liver tissues. The percentages of positive cells were counted within five microscopic fields under a ×20 objective lens for statistical analysis. *P<0.05, **P<0.01, ***P<0.001. Original magnification: ×100, bar: 50 µm. Ad5F11, chimeric fiber coding sequence of Ad5 and Ad11; Ad5H48 hexon, chimeric hexon coding sequence of Ad5 and Ad48; CAR, coxsackievirus–adenovirus receptor; FCM, flow cytometry; FITC-A, Fluorescein Isothiocyanate-A; GFP-A, Green fluorescent protein-A; HCC, hepatocellular carcinoma; MOI, multiplicity of infection; PBMC, peripheral blood mononuclear cell; PE-A, phycoerythrin-A; qRT-PCR, quantitative reverse transcription PCR; wAd5, wild-type Ad5.

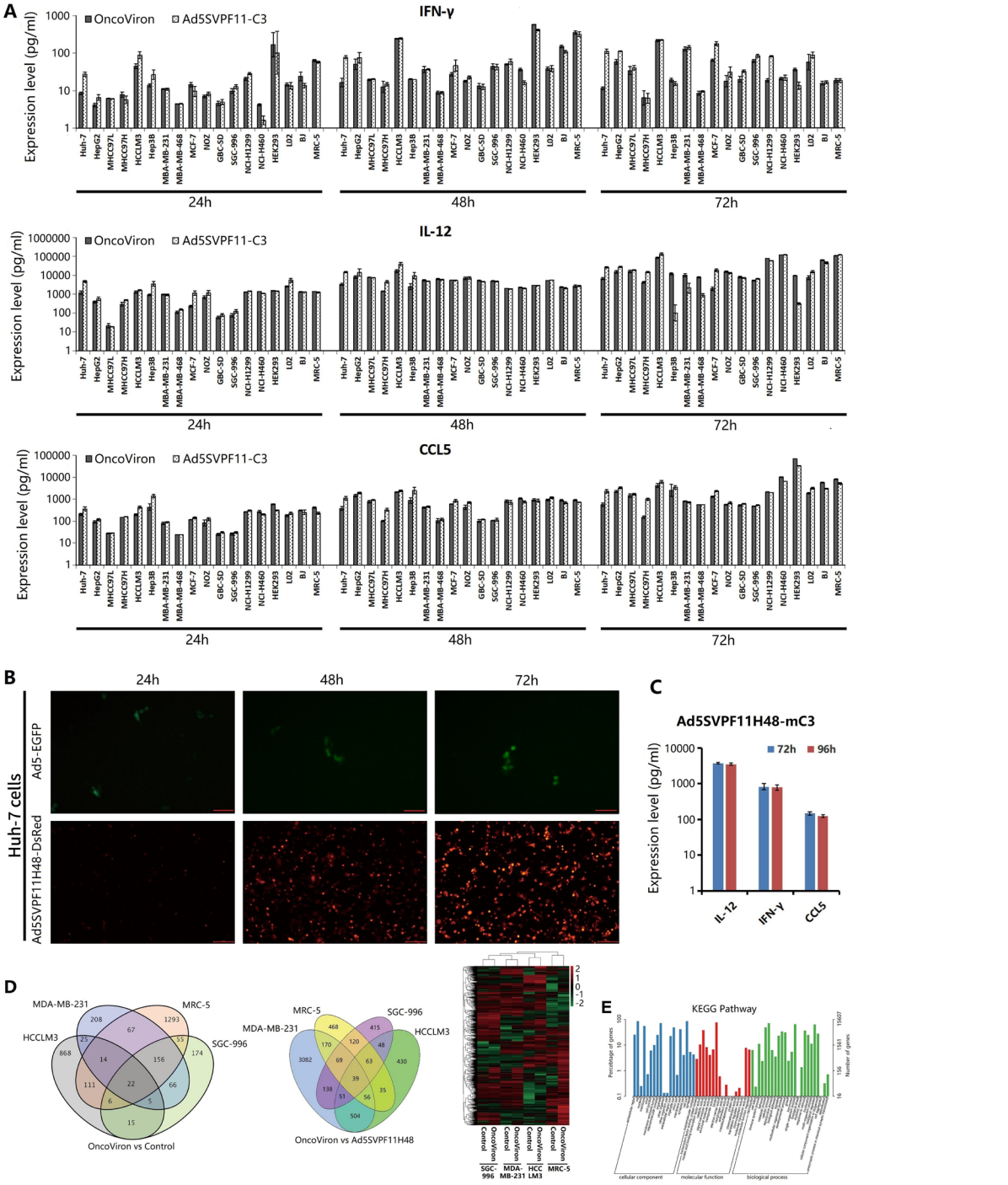

Figure 3 OncoViron and its control viruses mediated high expression of anticancer cytokines and their effects on cell transcriptional profile. (A) Cells were seeded in six-well plates, 5×10^5 cells/well, and cultured for 24 hours. OncoViron and Ad5SVPF11-C3 were infected at MOI=5 pfu/cell. Supernatants were collected at 24, 48, and 72 hours, respectively. The contents of IFN-γ, IL-12, and CCL5 were determined by ELISA. Bar: 200 µm. See also online supplemental figure S3B. (B) Fluorescent protein reporter gene expression assay. Huh-7 cells were cultured in 96-well plates, 1×10^4 cells/well, and infected with Ad5SVPF11H48-DsRed and Ad5-EGFP at MOI=5 pfu/cell. The expression intensity of DsRed and EGFP was observed under a microscope 24, 48, and 72 hours later. (C) Ad5SVPF11H48-mC3 carrying three murine cytokines efficiently expressed mIFN-γ, mIL-12 and mCCL5 in HEK293 cells. (D) Cell lines were cultured in six-well plates, 5×10^5 cells/well. After 24 hours' culture, OncoViron, Ad5SVPF11H48, Ad5SVPF11, Ad5SVPF11–IL12, Ad5SVPF11–CCL5, and Ad5SVPF11–IFNγ were infected at MOI=5 pfu/cell. The transcriptome sequencing analysis was performed 48 hours later, as well as functional annotation and enrichment analysis. Venn plots and expression level clustering of OncoViron induced changes in the number of DEGs in cells compared with the blank control group and blank virus group. (E) KEGG analysis of DEG pathways enriched cellular processes and environmental information processing between the OncoViron and control groups. CCL5, chemokine RANTES gene; DEG, differentially expressed gene; ELISA, enzyme linked immunosorbent assay; IFN-γ, interferon-γ; IL-12, interleukin 12; KEGG, Kyoto Encyclopedia of Genes and Genomes; MOI, multiplicity of infection.

HCCLM3, MDA-MB-231, and SGC-996 cells was different (online supplemental figure S3D), but the changes in cell function and signaling pathways were very similar among different cancer types.

After miRNA sequencing and screening, functional annotation and enrichment analysis of differentially expressed miRNA target genes were carried out by setting a threshold DESeq2_EBSeq FDR=0.05 FC=2. The results showed that OncoViron, Ad5SVPF11H48, Ad5SVPF11, Ad5SVPF11-IL12, Ad5SVPF11-CCL5, and Ad5SVPF11-IFNγ all caused changes of miRNA expression profiles in HCCLM3, MDA-MB-231, SGC-996, and MRC-5 cell lines (online supplemental table S3). The KEGG pathway enrichment analysis of differentially expressed miRNA target genes showed that the related genes were more enriched in endocytosis (online supplemental figure S3E).

OncoViron induces cancer-selective killing activity

Real-time cellular analysis showed that OncoViron, Ad5SVPF11-C3, Ad5SVPF11H48-DsRed, and Ad5SVPF11-DsRed had significant cytotoxic effects on various solid tumor cell lines with dose–effect and time–effect manners (figure 4A). CCK-8 assay on cell viability further reinforced that the series of OAVs presented an effective inhibitory effect on a variety of solid tumor cells. OncoViron chimerized with three serotypes of adenoviruses showed greater oncolytic activity than Ad5SVPF11-C3 chimerized with two serotypes in most cancer cell lines (figure 4B). These OAVs had a limited effect on normal BJ cells, requiring an extremely high MOI to exert a 50% killing effect (figure 4C). Comparing the IC50 values of the OAVs (Ad5SVPF11-DsRed and Ad5SVPF11H48-DsRed) and the replication-deficient adenovirus Ad5-EGFP, we found the results showed that Ad5-EGFP needed higher MOIs to exert the inhibitory effect on cancer cells (online supplemental figure S3F).

OncoViron exerts anticancer activity in animal implanted tumor models

OncoViron and its OAV counterparts demonstrated good anticancer activity against a variety of solid tumors (figure 5A and online supplemental figure S4A). In general, OncoViron was superior to Ad5SVPF11-C3 in nude mouse models of solid tumors, suggesting Ad5H48 chimerization enhanced the anticancer efficacy (figure 5Aa,b). Increased OncoViron dose could improve the efficacy (figure 5Ac,d,f). Ad5SVPF11-C3 carrying three cytokines was superior to the viruses carrying single or double cytokines, and even better than the blank viruses (figure 5Ab,d,e). In the subcutaneous xenograft model of MDA-MB-231 in NCG-hIL15 humanized mice transfused with human PBMCs, OncoViron completely inhibited tumor growth, and the tumor inhibition rate (TIR) reached 97.57% in the high-dose group (figure 5Ad). However, the model initially contained six animals in each group, and at 38 days after treatment, two mice in each of the OncoViron-treated groups and one mouse in each of the other groups died, which was most likely associated with PBMC-derived graft-versus-host disease (GVHD). In the immunocompetent mouse models of CT26 and B16 tumors, due to the immune-enhancing effects of the three human cytokines expressed by OncoViron and the three murine cytokines expressed by Ad5SVPF11H48-mC3, the efficacy of viral intratumoral injection was phenomenal and even significantly inhibited the growth of contralateral tumors that were not directly treated (figure 5Af,g). In the SGC-996 model, the TIRs of the blank virus Ad5SVPH48 group and three cytokine protein group were 24.03% and 15.26%, respectively. Compared with the TIR of 49.47% of the OncoViron medium dose group, the statistical Q value of the drug synergy was 1.39, confirming that OncoViron exerted synergistic efficacy of viral oncolytic and cytokine anticancer effects (figure 5Ac). During the observation period, except for a decrease of body weight and appearance of death in the MDA-MB-231 model mice transfused with PBMC and treated with OAVs, the body weight of other model mice continued to gradually increase with no statistical difference between any two groups (online supplemental figure S4B), and there were no abnormal changes in the life status of mice. The preliminary results showed that OncoViron had no obvious toxicity and side effects.

Immunohistochemistry showed that large areas of necrosis appeared after OncoViron treatment in tumor tissues of the nude mouse SGC-996 model. In the control group, survivin was strongly positive and distributed in the cytoplasm and nuclei, while survivin was reduced and the positive substances were mainly distributed in nuclei in the virus-treated groups. This result was related to OncoViron destroying the survivin-positive cancer cells and survivin in residual cancer cells transferred into nuclei (figure 5B). Compared with the control group, OncoViron-treated cancer cells were positive for E1a and hIFN-γ, and the percentage of Akt and p-Akt positive cells decreased; especially the p-Akt:Akt ratio decreased from 0.8908 in the control group to 0.2171 in the OncoViron group ($p<0.0001$). These phenomena are all molecular events that decrease the proliferation activity and survival of cancer cells, suggesting that the malignancy of residual cancer cells was reduced. In the B16 immunocompetent mouse model, OncoViron, Ad5SVPF11-mC3, and Ad5SVPF11H48-mC3 mediated E1a expression in cancer cells, and mIFN-γ in cancer cells were positive in the Ad5SVPF11-mC3 and Ad5SVPF11H48-mC3 groups. The number of CD3+, CD4+ and CD8+ T cells in TME increased significantly in the OncoViron and Ad5SVPF11H48-mC3 groups compared with the control group, but OncoViron was not as strong at chemotactic immune cells as Ad5SVPF11H48-mC3 (figure 5C). These results suggested that after OncoViron and Ad5SVPF11H48-mC3 treatments, not only the proliferation activity of cancer cells decreased, but also the number of infiltrating immune cells increased, demonstrating the tumor immune microenvironment was significantly changed.

OncoViron synergistically inhibits tumor growth when combined with immunotherapy in animal implanted tumor models

OncoViron was tested for anticancer activity in a human pharyngeal squamous cell carcinoma FaDu subcutaneous

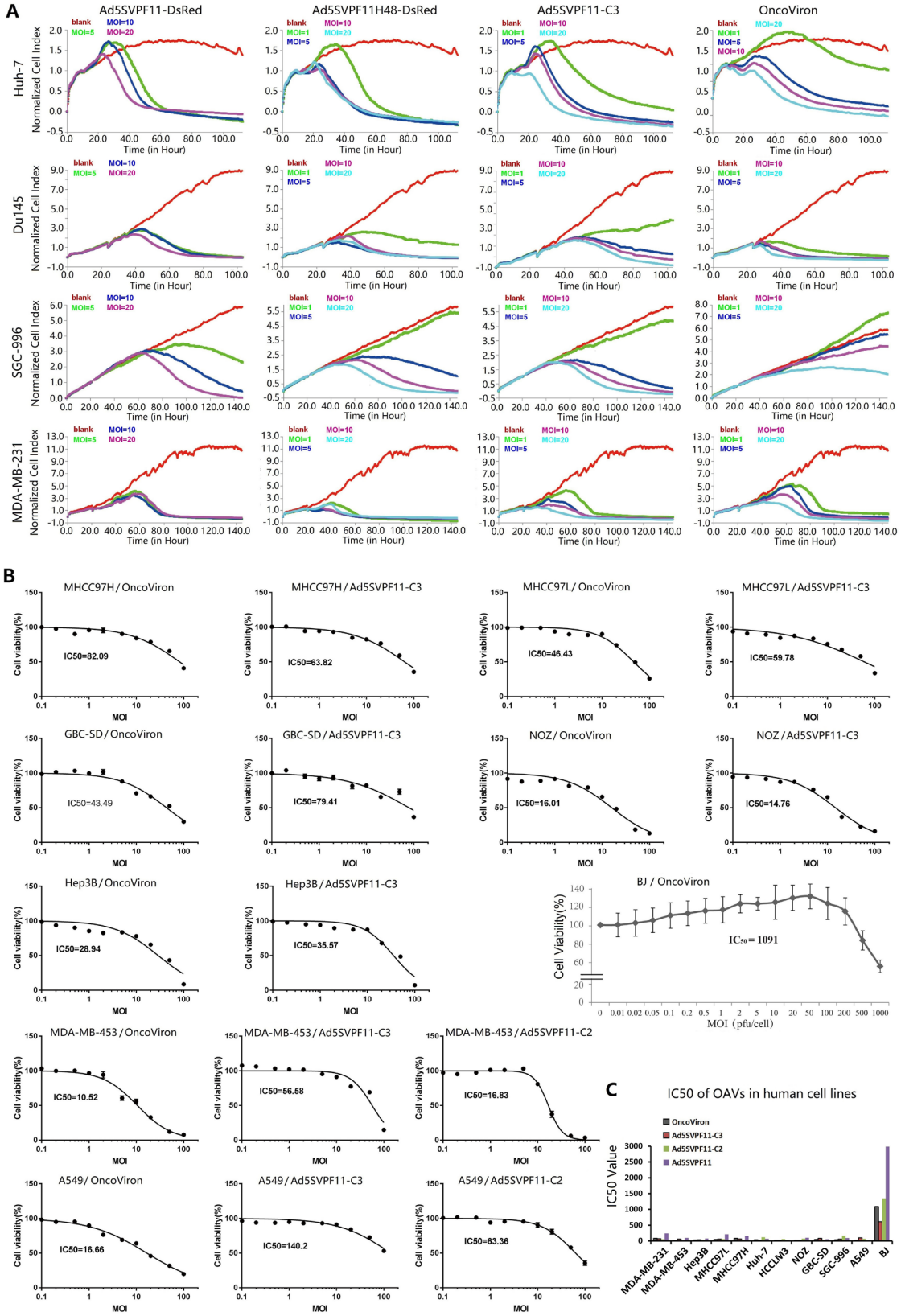

Figure 4 Selective killing activity of OAVs in experimental cell lines. (A) Cells were cultured in 16-well E-plates at 5×10^3 cells/well. After 24 hours of culture, viruses were infected at MOI=0, 1, 5, 10, and 20 pfu/cell; cell proliferation was dynamically observed by RTCA and recorded cell index data. (B) CCK8 assay was used to detect the killing effect of viruses on cells. Cells were cultured in 96-well plates, 1×10^4 cells/well, and infected with viruses at a gradient of MOIs. After 7 days of culture, CCK8 solution was added; the light absorption value at 490 nm was measured with a microplate analyzer; cell viability was detected; and IC50 values were calculated. (C) Comparison of IC50 values of killing effect of OAVs. MOI, multiplicity of infection; OAV, oncolytic adenovirus; RTCA, real-time cellular analysis.

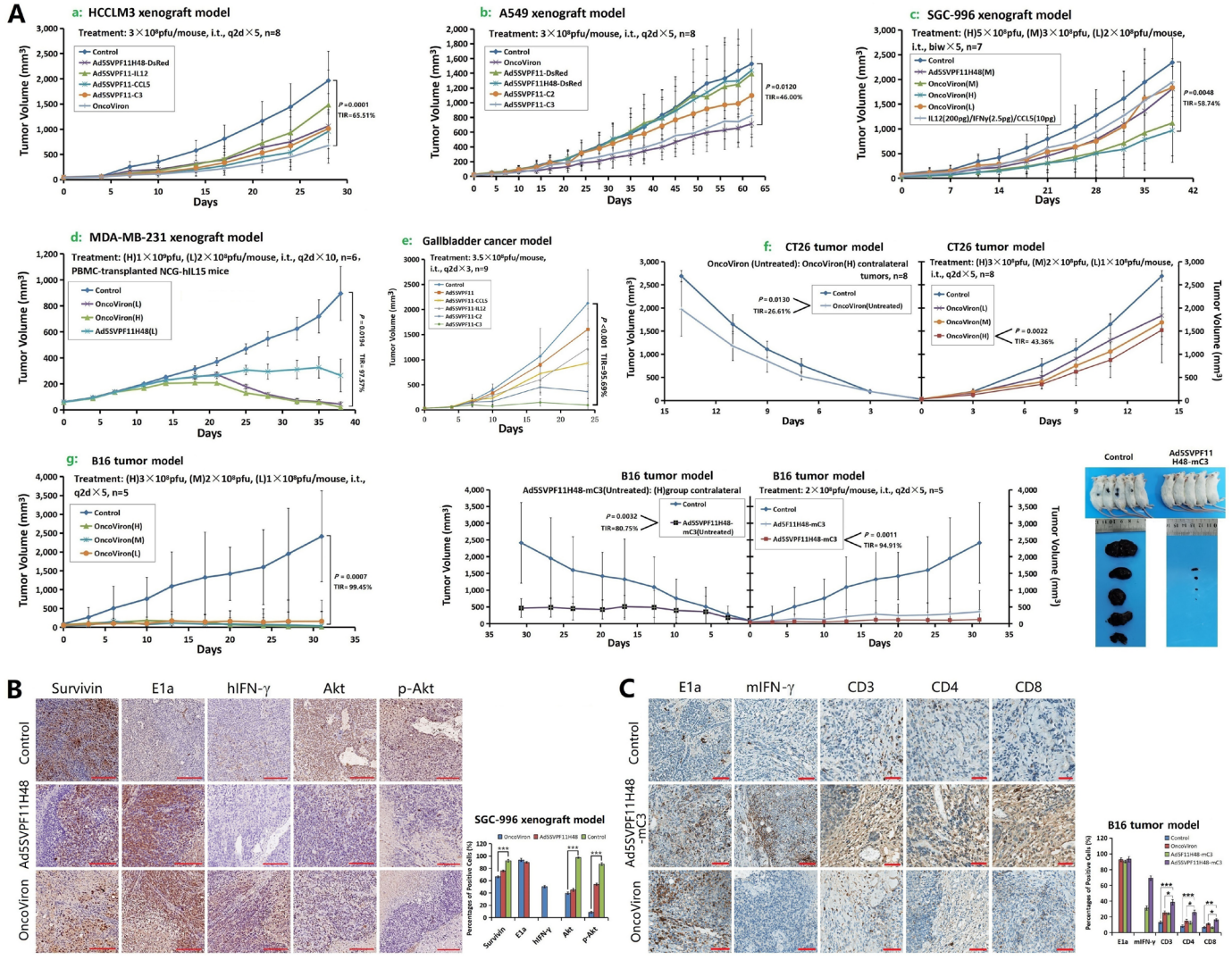

Figure 5 Anticancer activity of OncoViron and its control viruses in mouse implanted tumor models. (A) 1×10^6 cells to 1×10^7 cells per mouse according to its tumor-forming ability, or 1 mm^3 tumor tissues, were injected subcutaneously in the axillary of mice. When the tumor was about 3.0–5.0 mm in diameter, mice were grouped and treated with different doses of viruses. After treatment, tumor size was measured regularly, and the formula of 'maximum diameter×minimum diameter×minimum diameter×0.5' was used to calculate tumor volume. (A–E) Nude mouse xenograft models of the indicated human cancers. (D) PBMC-humanized NCG-hIL15 mouse model of MDA-MB-231 cell xenografts. (F) Immunocompetent mouse models of murine CT26 cells. (G) Immunocompetent mouse models of murine B16 cells. (B) Immunohistochemical detection of SGC-996 xenograft tumor tissues in nude mice. Original magnification: ×40, bar: 200 µm. (C) Immunohistochemical detection of murine B16 tumor tissues in immunocompetent mouse models. Original magnification: ×100; bar: 50 µm. *P<0.05, **P<0.01, ***P<0.001. PBMC, peripheral blood mononuclear cell; TIR, tumor inhibition rate.

tumor model in PBMC-humanized mice. OncoViron at a low dose was more effective than Keytruda in tumor suppression, and the efficacy of OncoViron was significantly enhanced when in combination with Keytruda (figure 6A). The PBMC-humanized NCG-hIL15 mice also died during the observation period, with initially seven animals in each group, at day 18 after treatment, one death in each of the blank control group, OncoViron low-dose group, and Keytruda group, and two deaths in each of the other three groups. It was predicted that animal death may be associated with GVHD.

The efficacy of Ad5SVPF11H48-mC3 combined with PD-1 antibody was tested in the implanted tumor model of murine colon cancer MC38 in C57-hPD1-humanized mice. The TIRs of Ad5SVPF11H48-mC3 (G2 group), Keytruda (G3 group), and Ad5SVPF11H48-mC3+Keytruda (G4 group) were 18.71%, 69.05%, and 88.86%, respectively, at 18 days after the first treatment. The Q value of drug synergy was 1.19, confirming that the combination of Ad5SVPF11H48-mC3 and Keytruda had synergistic effect (figure 6B). Single-cell transcriptome sequencing was performed for the MC38 tumors, and in total, five clusters of cell types were identified through clustering analysis by UMAP (uniform manifold approximation and projection) dimensional reduction and classical cell type marker genes. Top25 heat map showed changes in gene expression profiles (figure 6C). The number and location of cancer cells in the G4 group were changed,

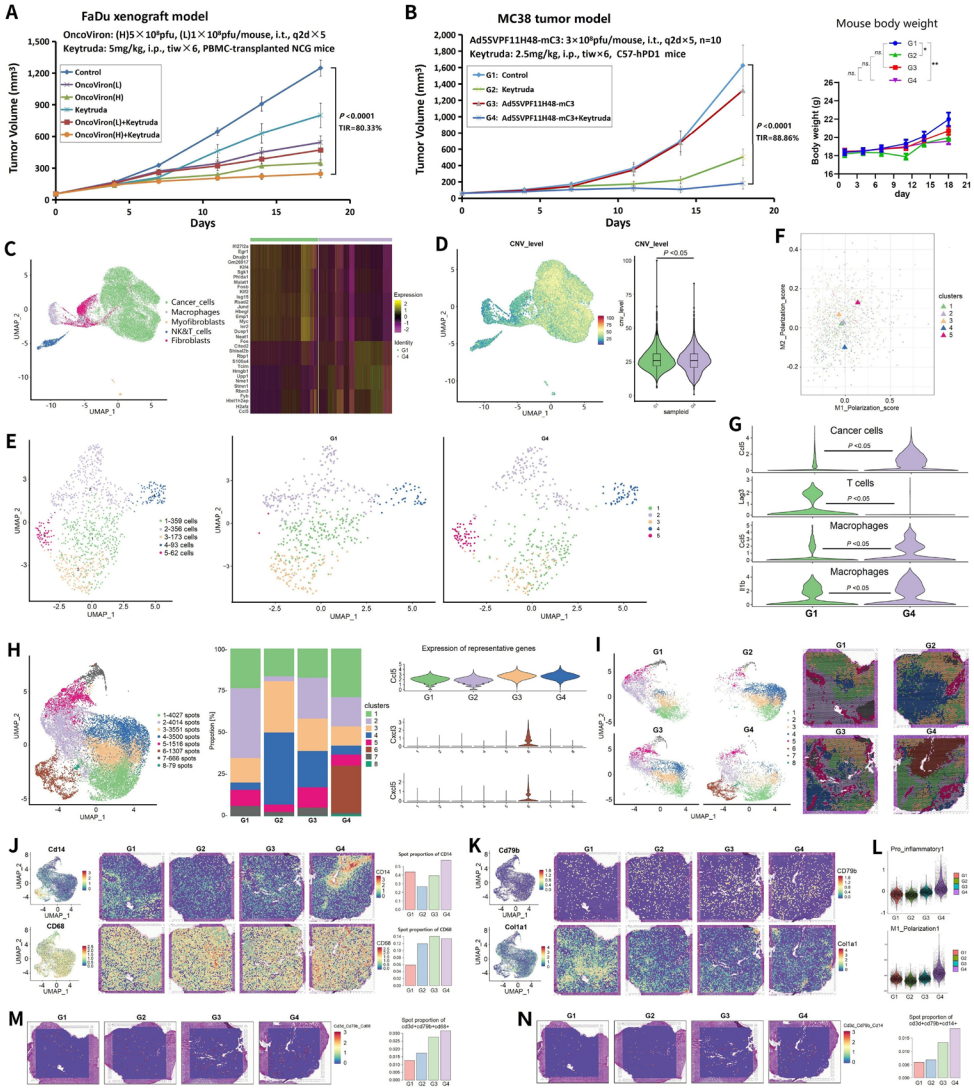

Figure 6 Synergistic anticancer effect of OncoViron combined with PD-1 antibody on animal implanted tumor models. (A) PBMC-humanized NCG mouse model of human pharyngeal squamous cell carcinoma. FaDu cells were injected in the right axillary of NCG mice at 5×10^6 cells per mouse. At 8 days after inoculation, PBMCs were intravenously injected into mice at 2×10^6 cells per mouse. After tumor formation, mice were intratumorally injected with OncoViron at 5×10^8 pfu/mouse and 1×10^8 pfu/mouse in high and low doses of OncoViron, respectively, once every other day, five times. Mice in the Keytruda group were injected intraperitoneally with Keytruda at 5 mg/kg/mouse, two times a week for 3 weeks. The blank control group was simultaneously given VPS of 100 µL per mouse each time. Tumor size was measured regularly and tumor volume was calculated. (B) C57-hPD1-humanized mouse model of murine colon cancer cell MC38 cells. The Ad5SVPF11H48-mC3 group was intratumorally injected with viruses at a dose of 3×10^8 pfu/mouse, once every other day, five times. Keytruda was intraperitoneally injected in the Keytruda group and the Ad5SVPF11H48-mC3+Keytruda group, 2.5 mg/kg/mouse, two times a week for 3 weeks. *P<0.05, **P<0.01. (C) Single-cell transcriptomic profiling was performed for MC38 tumors in the Ad5SVPF11H48-mC3+Keytruda group (G4) compared with the control group (G1). UMAP plot colored by cluster (left) and Top25 heatmap of the expression of DEGs (right) between two groups. (D) UMAP and violin map of CNV levels between G1 and G4 groups. (E) UMAP plot of macrophages colored by cluster. (F) M2/M1 polarization score of macrophage clusters. (G) Representative DEGs in cancer cells (CCL5), T cells (Lag3) and macrophages (CCL5 and Il1b). (H) Spatial transcriptomic profiling for MC38 tumors in the hPD-1 humanized mouse model. UMAP of changes in the number of eight cell-type clusters among G1 to G4 groups, and the differentially expression of the representative DEGs (eg, CCL5 highly expressed in G3 and G4 groups, and CXCL3 and CXCL5 high expression in cluster 6). (I) UMAP of eight cell-type clusters and spatial transcriptomic feature plots from representative sections among G1–G4 groups. (J) UMAP plots of CD14+ and CD68+ cells, spatial transcriptomic feature plots and spot proportion among G1–G4 groups. (K) UMAP plots of CD79b+ and Col1a1+ cells, and spatial transcriptomic feature plots among G1–G4 groups. (L) Enrichment of proinflammatory genes and M1 polarization levels among the four groups. (M) Spatial colocalization of CD3d+ T cells, CD79b+ B cells and CD68+ macrophages and spot proportion among the four groups. (N) Spatial colocalization of CD3d+ T cells, CD79b+ B cells and CD14+ mononuclear macrophages and spot proportion among the four groups. CCL5, chemokine RANTES gene; CNV, copy number variation; DEG, differentially expressed gene; ns, no significance; PBMC, peripheral blood mononuclear cell; TIR, tumor inhibition rate; UMAP, uniform manifold approximation and projection; VPS, virus preservation solution.

and the increase of fibroblasts was significant (online supplemental figure S4C). The cell subsets altered significantly and the copy number variation (CNV) level of cancer cells in different cell populations was higher (online supplemental figure S4D,E), and the overall CNV level in the G4 group was lower than that in the G1 group (figure 6D). Macrophages in TME were divided into five clusters, among which cluster 5 was significantly increased in the G4 group and expressed CD14 at the highest level, while Lcn2, Il1a, Cxcl3, etc, were upregulated (figure 6E and online supplemental figure S4F). Cluster 5 in the G4 group also showed obvious M1 characteristics (figure 6F). In the G4 group, except for the high expression of CCL5 in cancer cells, Lag3 in T cells was significantly downregulated (figure 6G). The increased expression of CCL5 and Il1a in macrophages, as well as the changes of transcriptional factor interaction and HIF-1 signaling pathway regulation (online supplemental figure S4G), further indicated the transformation of macrophages from M2 to M1. The reclustering analysis of NK&T cells showed that the number of cluster 7 with natural killer (NK) cell characteristics increased in the G4 group (online supplemental figure 4H,I). A total of eight cell clusters were identified by spatial transcriptome analysis of tumors in the MC38 model. Cluster 2 in each of the treatment groups decreased compared with the G1 control group, while cluster 6 significantly increased. In addition to the high expression of virus-mediated CCL5 in the G3 and G4 groups, CXCL3 and CXCL5 in cluster 6 were significantly upregulated (figure 6H,I, and online supplemental figure S5A), and Igkc and Saa3 in the cluster eight were upregulated in all treatment groups (online supplemental figure S5B). Cluster 2 showed high activity for hypoxia response, oxidative phosphorylation process, and HIF-1 signaling pathway, while cluster 6 showed high activity for TNF response, inflammatory response process, and NF-κB, IL-17, PI3K/Akt, and TNF signaling pathways (online supplemental figure S5C). Consistent with the single-cell sequencing results, spatial transcriptome analysis also found an increase in the number of CD68+ macrophages in the treatment groups, especially focal aggregation of CD14+ mononuclear macrophages in the G4 group (figure 6J), and an increase in CD79b+ B cells accompanied by a decrease in collagen production in stroma (figure 6K). The G4 sample had high proinflammatory activity and M1 polarization was more obvious (figure 6L). Colocalization of CD3d+ T cells, CD79b+ B cells, and CD14+ mononuclear macrophages, as well as colocalization of CD3d+ T cells, CD79b+B cells, and CD68+ macrophages, showed that those cells were significantly increased in the two groups treated with OncoViron (figure 6M,N). Immunohistochemistry showed that in the same region where OncoViron was distributed and expressed mE1a, a large area of cancer tissue necrosis was observed, accompanied by aggregation of lymphocytes, mononuclear macrophages, dendritic cells (DCs), and fibroblasts, forming a third lymphoid structure in TME (online supplemental figure S5D), which exerted an in situ synergistic killing effect on cancer cells, thus enhancing the curative efficacy with immunotherapy.

We prepared chimeric antigen receptor (CAR) T cells and demonstrated that neither OncoViron nor Ad5SVPF11H48-DsRed affected CAR T-cell proliferation (figure 7A) and cancer killing ability (figure 7B). On the prostate cancer Du145 and breast cancer MDA-MB-231 xenograft models in NCG mice, OAVs combined with CAR T cells showed an enhanced tumor suppression effect (figure 7C,D). OncoViron had a TIR of 80.19% ($p<0.0001$ vs control group), and OncoViron+CAR T group had a higher TIR of 97.56% ($p<0.0001$ vs control group) in the Du145 model, and the MDA-MB-231 model also showed prolonged survival in all OAV+CAR T groups (figure 7E). FCM confirmed that the combination of Ad5SVPF11-C3 and OncoViron expressing three cytokines significantly prolonged CAR T survival and increased the number of CAR T cells in blood (figure 7F,G, and online supplemental figure S6). By comparison, Ad5SVPF11-C3 promoted CAR T proliferation more strongly than OncoViron. In terms of efficacy, OncoViron was significantly better than Ad5SVPF11-C3 when they were used alone ($p<0.05$), whereas Ad5SVPF11-C3 was slightly better than OncoViron when combined with CAR T therapy in both models ($p>0.05$). The inversion of this result could be caused by Ad5SVPF11-C3 being more likely to promote CAR T proliferation and survival than OncoViron. An increased number of hCD45-positive CAR T cells infiltrated in tumor tissues in the OncoViron+CAR T group (figure 7H,I). OncoViron did indeed promote CAR T cell proliferation and infiltration, forming a synergistic mechanism that significantly improved the therapeutic effect.

DISCUSSION

Oncolytic virotherapy has been considered as a branch of immunotherapy.[13] Although many types of viruses can be modified into OVs, adenoviruses are so far the best choice for development of highly potent OVs with multiple mechanisms of synergistic anticancer activity due to their wide range of target cells, no risk of genome integration mutagenesis, large genome size, and ease to produce in large quantities.[14] One of the mechanisms to achieve OAV-selective replication within tumor cells is to place adenovirus E1a expression under the control of a tumor-specific promoter. Through previous studies on the specificity of survivin expression in various cancers[15–19] and the elucidation of the functional role of the HIF-1α ODD domain,[20] we selected the survivin promoter as a regulatory element for OAV broad-spectrum cancer targeting to enhance viral specific replication activity at the transcriptional level and the fusion of ODD within E1a protein as a genetic ON/OFF switch to ensure that E1a is degraded under normoxia in normal tissues, which can inhibit viral replication in normal cells at the translational level. At the same time, knockdown of Elb-55kD allows OAVs to maintain their capacity to replicate in tumor cells while sparing normal

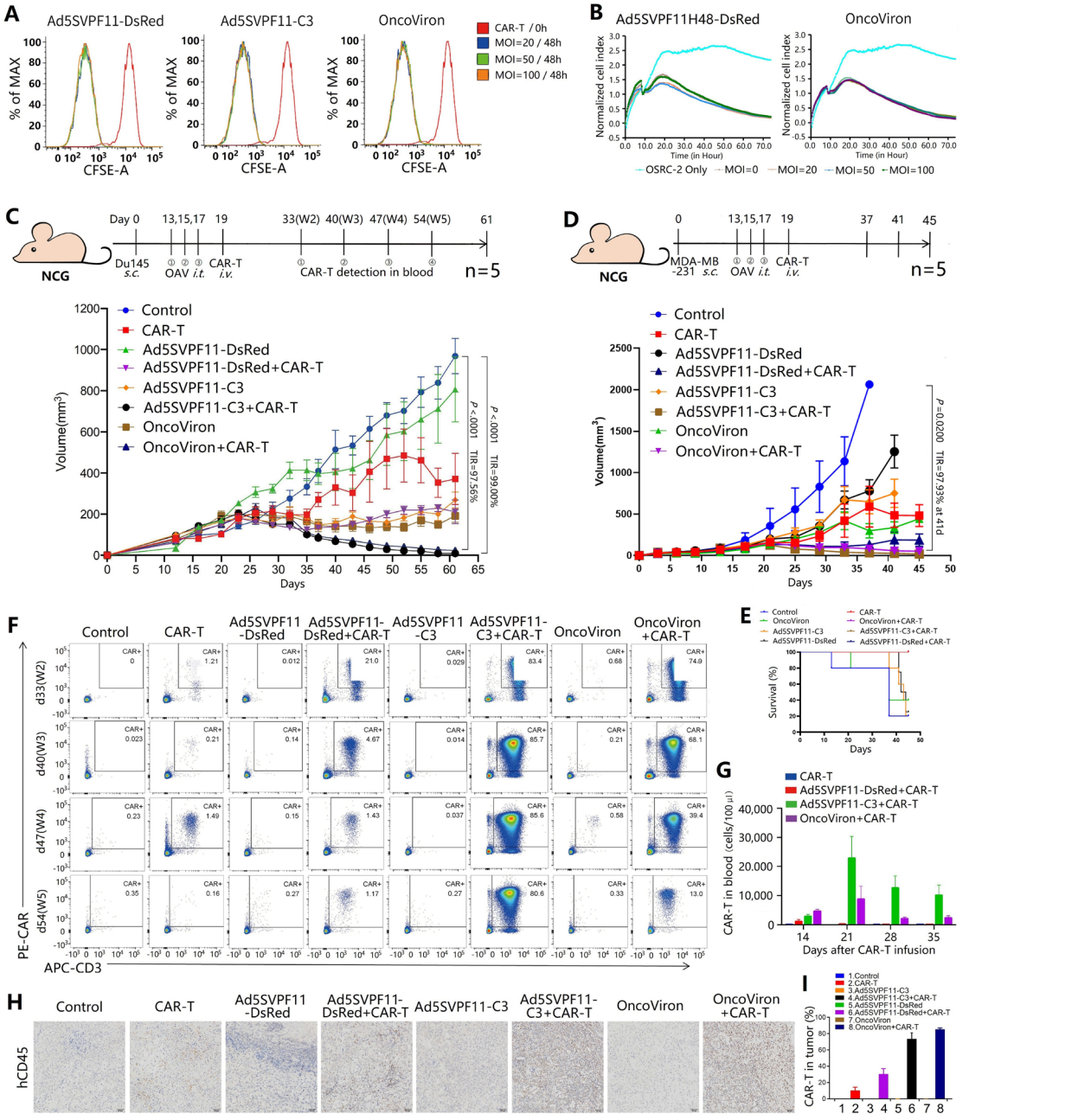

Figure 7 Synergistic anticancer effect of OncoViron combined with CAR T cells on animal xenograft tumor models. (A) The prepared 1×10^7 CAR T cells were collected and seeded in 24-well plates at 1×10^6 cells/well. The viruses, OncoViron, Ad5SVPF11-C3 and Ad5SVPF11H48-DsRed were added at a gradient of MOIs, and cells were collected 48 hours later and stained with CFSE, then fluorescence intensity was detected by FCM and compared with that of the initial CAR T cells. (B) Kidney cancer OSRC-2 cells were inoculated into RTCA-specific culture plates. After cell adherence, CAR T cells were added at the effect:target ratio of 1 (CAR T:OSRC-2=1:1), and the viruses Ad5SVPH48-DsRed and OncoViron were added at a gradient of MOIs, and the killing activity of viruses on OSRC-2 cells was monitored by RTCA. (C) NCG mice were subcutaneously inoculated with Du145 cells, 3×10^6 cells per mouse. Mice were divided into groups when tumor formation reached about 80 mm^3. In the virus treatment groups, a total dose of 1×10^9 pfu viruses was intratumorally injected three times, once every other day. After the second day when finishing virus injections, CAR T cells were injected into the tail vein, 2×10^6 cells/200 µL/mouse. The same volume of PBS was simultaneously injected to mice in the blank control group. Tumor size was measured regularly. (D) MDA-MB-231 model in NCG mice was established and treated with OAVs combined with CAR T cells. (E) The survival curve of the MDA-MB-231 model. (F) In the Du145 model, peripheral blood of mice was collected at 14 (W2), 21 (W3), 28 (W4), and 35 (W5) days after CAR T infusion, or 33, 40, 47, and 54 days after cancer cell inoculation, and the contents of CAR T cells were detected by FCM. (G) Histogram of the contents of CAR T cells in blood of Du145 model mice. (H) After the end of the experiment, Du145 tumor tissues were collected, and the infiltrated hCD45+ CAR T cells in the tumor tissues were detected by immunohistochemistry. Original magnification: ×40, bar: 50 µm. (I) Histogram of the percentages of hCD45+ CAR T cells in Du145 tumor tissues. CAR, chimeric antigen receptor; CFSE, carboxyfluorescein diacetate succinimidyl ester; MOI, multiplicity of infection; OAV, oncolytic adenovirus; PBS, phosphate buffered solution; RTCA, real-time cellular analysis.

cells.[21] OncoViron with the triple-regulatory mechanism was found to replicate in high copies in many solid tumor cell lines such as liver, breast, gallbladder, and lung cancers, while their replication activity was generally low in normal cell lines. On the other hand, the elevated expression of hypoxia-inducible factor HIF-1α in solid tumors regulates the transcription of a range of downstream target genes, facilitating tumor energy metabolism under hypoxic conditions, stimulating angiogenesis and tumor growth. HIF-1α protein has an internal ODD, which controls the degradation of HIF-1α through the ubiquitin/proteasome cascade. Under hypoxic environment of tumor tissues, the HIF-1α protein is protected by ODD and remains stable, inducing the expression of a series of downstream genes that promote tumor growth and metastasis.[22] Within OncoViron, a fusion of ODD with E1a protein was designed so as to protect E1a from degradation in TME hypoxic environment, thus exerting a viral replicative effect, whereas E1a was degraded in normal tissue under normoxia to prevent virus replication. Our cytological experiments confirmed that the hypoxia-dependent OAVs could initiate the rigorous, conditional replication within cancer cells and avoid damaging normal cells. Thus, our designed cancer-targeting triple-regulation mechanism achieved the expected safety and efficacy guarantees.

OAV preserves the expression of E1a protein, which itself has an anticancer effect,[23] and E1a mutation can further release or enhance the anticancer activity.[24] Particularly, reasonably deleting part of the E3 region during OAV construction freed viral loading capacity and facilitated viral replication and long-lasting gene expression.[25] Among the 52 serotypes of six groups of human adenovirus family, Ad11 in group B recognizes a widely expressed complement regulatory protein, CD46, as its receptor. Replacing Ad5 fiber knob with Ad11 fiber knob to construct chimeric Ad5F11 fiber will enable OAV to also recognize CD46. Theoretically, this could lead to complete eradication of the source of tumor recurrence.[26] The expression level of CD46 is higher than CAR in multiple types of cancer cell lines. The Ad5F11-chimeric OAV had a significantly improved infection activity among various types of cancer cells, especially tumor stem cells with lack of CAR expression. In addition, Ad5 is widely found in nature; most people are already infected and have a neutralizing antibody that can intercept therapeutic Ad5 vectors, therefore diminishing the treatment efficacy. Adenovirus capsid protein hexon is the main antigen to stimulate neutralizing antibody production.[27] To help OAVs evade interception of preexisting immunity, we selectively chimerized seven HVRs in Ad5 hexon with the hexon of a rare serotype Ad48 in group D to form a chimeric hexon Ad5H48; the Ad5H48-chimeric OAV effectively resisted interception by neutralizing antibodies produced by wAd5 pre-treatment in mice. Thus, the triple chimerization endowed OncoViron with greater infectivity and viability.

Using OAV as a vector for the transfer of anticancer genes can facilitate the high copy replication and efficient expression of anticancer genes specifically in cancer cells. We loaded three anticancer genes in the adenovirus E3 region, including two immune-enhancing cytokine genes (IL-12 and IFN-γ) and one immune cell chemokine gene (CCL5), all of which have active and direct synergistic mechanisms with the therapies of immune checkpoint inhibitors and CAR T/CAR NK cells. During immunotherapy with PD-1/PD-L1 antibodies, the synthesis and secretion of IFN-γ and IL-12 by DCs trigger T-cell killing activity.[28] However, DCs are often lacking; IFN-γ and IL-12 are not secreted in sufficient amounts in solid tumor TME. When OAV is loaded with IL-12 and IFN-γ and combines with PD-1 antibody, OAV-mediated cytokine expression can directly activate killer T cells within TME, rapidly making PD-1 antibody to exert anticancer efficacy. When in combination with CAR T/CAR NK therapy, OAV-expressed IL-12 prolongs the survival of CAR T/CAR NK cells and IFN-γ enhances CAR T/CAR NK killing activity. Of course, IL-12 and IFN-γ themselves have strong anticancer activities.[29 30] OAV is loaded with chemokine CCL5, which can recruit T cells, NK cells, macrophages, and other immune cells to migrate and accumulate in TME.[31 32] When OAV is combined with PD-1 antibodies, CCL5 increases the number of tumor-infiltrating leukocytes (TILs) in TME, synergistically enhancing the killing effect on cancer cells.[29 33] When combined with CAR T/CAR NK, CCL5 not only attracts more CAR T/CAR NK cells into TME but also promotes the synergistic enhancement of CAR T/CAR NK function with other recruited TILs, T cells, NK cells, and macrophages. It was demonstrated that, along with the selective replication of OncoViron and the expression of anticancer cytokines, the specific killing effect of OncoViron on cancer cells was fully presented and caused a significant change in gene expression profile in cancer cells. Thus, the triple-transgene loading in OAV had a significant killing effect on a variety of solid tumors.

In order to verify the broad-spectrum anticancer effect and mechanism of OncoViron, we established implanted tumor models in immunodeficient mice, immunocompetent mice, and humanized mice, and the animal experiments confirmed that OncoViron exhibited better anticancer activity against a variety of solid tumors. In the C57-hPD1 humanized mouse model of murine colon cancer MC38 cells, OncoViron in combination with PD-1 antibody (Keytruda) showed synergistic anticancer efficacy. In the NCG mouse model of human prostate cancer Du145 cells, OncoViron combined with CAR T-cell therapy had highly significant therapeutic effects; the expressed cytokines prolonged the survival of CAR T and promoted CAR T-cell proliferation and infiltration in TME. Single-cell sequencing and spatial transcriptome analysis of animal tumor specimens confirmed that OncoViron

could not only recruit a large number of NK, T cells, and macrophages to enter into TME but also activate those immune cells, thus reprogramming TME and creating favorable conditions for combination therapy. Although the safety of OncoViron was not assessed in this study, it has been confirmed by in vitro assays that OncoViron targets tumor cells strictly and by in vivo animal studies that OncoViron has no effect on body weight and life status in mice, providing a preliminary indication that OncoViron is safe for use in cancer therapy. Its standardized safety evaluation study is in progress.

In conclusion, this study developed a novel OAV, OncoViron, which achieved significant improvement in both specificity and efficacy. OncoViron can be used as an immunotherapeutic synergist in combination with immune checkpoint inhibitor therapy and CAR T therapy, which will improve TME of solid tumors and amplify the effect of immunotherapy, thus broadening the scope of OAV application.

Author affiliations
[1]Department of General Surgery, Huashan Hospital, Cancer Metastasis Institute, Fudan University, Shanghai 200040, China
[2]National Center for Liver Cancer (NCLC), Navy Military Medical University, Shanghai 201805, China
[3]Department of Molecular Oncology, Eastern Hepatobiliary Surgery Hospital, Navy Military Medical University, Shanghai 200438, China
[4]Jiangsu Center for the Collaboration and Innovation of Cancer Biotherapy & Cancer Institute, Xuzhou Medical University, Xuzhou 221002, Jiangsu, China
[5]Department of Pathology, Second People's Hospital of Hefei, Hefei 230011, Anhui, China

Acknowledgements The authors thank Lixin Chen from Shanghai Laboratory Animal Center (Shanghai, China) for assistance in animal experiments. We also thank OE Biotech Co (Shanghai) for helping us in single-cell sequencing and spatial transcriptome analysis, OBio Technology Corp. (Shanghai) in adenovirus pilot production, NovelBio Bio-Pharm Technology Co. (Shanghai) in figure processing and assembly, and Biomarker Technologies Co. (Beijing, China) in transcriptome sequencing.

Contributors Conception and design: YS, JL, JZ, LQ, and CS; Development of methodology: YSu, JL, WJ, QZ, GW, LF, LA, SY, and LC; Acquisition of data: YS, JL, WJ, and QZ; Analysis and interpretation of data: JL, WJ, QZ, GW, and LF; writing of the original draft and/or revision of the manuscript: YS, JL, LQ, and CS; technical or material support: LC and MZ; supervision, funding acquisition, Funding acquisition and project administration: JZ, LQ, and CS. All authors contributed to review and agreed to the published version of the manuscript. CS is responsible for the overall content as the guarantor.

Funding This work was supported by the National Key R&D Program of China (2018YFA0900902), the Key project of National Natural Science Foundation of China (81930074), and the the National Natural Science Foundation of China (82002821).

Competing interests None declared.

Patient consent for publication Not applicable.

Ethics approval Not applicable.

Provenance and peer review Not commissioned; externally peer reviewed.

Data availability statement All data relevant to the study are included in the article or uploaded as supplementary information.

Supplemental material This content has been supplied by the author(s). It has not been vetted by BMJ Publishing Group Limited (BMJ) and may not have been peer-reviewed. Any opinions or recommendations discussed are solely those of the author(s) and are not endorsed by BMJ. BMJ disclaims all liability and responsibility arising from any reliance placed on the content. Where the content includes any translated material, BMJ does not warrant the accuracy and reliability of the translations (including but not limited to local regulations, clinical guidelines, terminology, drug names and drug dosages), and is not responsible for any error and/or omissions arising from translation and adaptation or otherwise.

Open access This is an open access article distributed in accordance with the Creative Commons Attribution Non Commercial (CC BY-NC 4.0) license, which permits others to distribute, remix, adapt, build upon this work non-commercially, and license their derivative works on different terms, provided the original work is properly cited, appropriate credit is given, any changes made indicated, and the use is non-commercial. See http://creativecommons.org/licenses/by-nc/4.0/.

ORCID iD
Changqing Su http://orcid.org/0000-0002-3396-7248

REFERENCES

1 Heidbuechel JPW, Engeland CE. Oncolytic viruses encoding bispecific T cell engagers: a blueprint for emerging immunovirotherapies. *J Hematol Oncol* 2021;14:63.
2 Proboka G, Tilgase A, Isajevs S, *et al*. Melanoma unknown primary brain metastasis treatment with ECHO-7 oncolytic virus Rigvir: a case report. *Front Oncol* 2018;8:43.
3 Wei D, Xu J, Liu X-Y, *et al*. Fighting cancer with viruses: oncolytic virus therapy in China. *Hum Gene Ther* 2018;29:151–9.
4 Ferrucci PF, Pala L, Conforti F, *et al*. Talimogene Laherparepvec (T-VEC): an intralesional cancer immunotherapy for advanced melanoma. *Cancers* 2021;13:1383.
5 Bernstock JD, Hoffman SE, Chen JA, *et al*. The current landscape of oncolytic herpes simplex viruses as novel therapies for brain malignancies. *Viruses* 2021;13:1158.
6 Nishio N, Dotti G. Oncolytic virus expressing RANTES and IL-15 enhances function of CAR-modified T cells in solid tumors. *Oncoimmunology* 2015;4:e988098.
7 Ribas A, Dummer R, Puzanov I, *et al*. Oncolytic virotherapy promotes intratumoral T cell infiltration and improves anti-PD-1 immunotherapy. *Cell* 2017;170:e10:1109–19.
8 Heise C, Sampson-Johannes A, Williams A, *et al*. Onyx-015, an E1B gene-attenuated adenovirus, causes tumor-specific cytolysis and antitumoral efficacy that can be augmented by standard chemotherapeutic agents. *Nat Med* 1997;3:639–45.
9 Yano S, Tazawa H, Kishimoto H, *et al*. Real-Time fluorescence image-guided oncolytic virotherapy for precise cancer treatment. *Int J Mol Sci* 2021;22:879.
10 Ramesh N, Ge Y, Ennist DL, *et al*. CG0070, a conditionally replicating granulocyte macrophage colony-stimulating Factor–Armed oncolytic adenovirus for the treatment of bladder cancer. *Clin Cancer Res* 2006;12:305–13.
11 Pokrovska TD, Jacobus EJ, Puliyadi R, *et al*. External beam radiation therapy and Enadenotucirev: inhibition of the DDR and mechanisms of Radiation-Mediated virus increase. *Cancers* 2020;12:798.
12 Kim SOY, Kang S, Song JAEJ, *et al*. The effectiveness of the oncolytic activity induced by Ad5/F35 adenoviral vector is dependent on the cumulative cellular conditions of survival and autophagy. *Int J Oncol* 2013;42:1337–48.
13 Melcher A, Harrington K, Vile R. Oncolytic virotherapy as immunotherapy. *Science* 2021;374:1325–6.
14 Ono R, Takayama K, Sakurai F, *et al*. Efficient antitumor effects of a novel oncolytic adenovirus fully composed of species B adenovirus serotype 35. *Molecular Therapy - Oncolytics* 2021;20:399–409.
15 Hu H, Li Z, Chen J, *et al*. P16 reactivation induces anoikis and exhibits antitumour potency by downregulating AKT/survivin signalling in hepatocellular carcinoma cells. *Gut* 2011;60:710–21.
16 Liu C, Sun B, An N, *et al*. Inhibitory effect of survivin promoter-regulated oncolytic adenovirus carrying p53 gene against gallbladder cancer. *Mol Oncol* 2011;5:545–54.
17 Li C, Yan Y, Ji W, *et al*. Oct4 positively regulates survivin expression to promote cancer cell proliferation and leads to poor prognosis in esophageal squamous cell carcinoma. *PLoS One* 2012;7:e49693.
18 Zhang Y, Fang L, Zhang Quan'an, *et al*. An oncolytic adenovirus regulated by a radiation-inducible promoter selectively mediates hSulf-1 gene expression and mutually reinforces antitumor activity of I131-metuximab in hepatocellular carcinoma. *Mol Oncol* 2013;7:346–58.
19 Su C. Survivin in survival of hepatocellular carcinoma. *Cancer Lett* 2016;379:184–90.
20 Li J, LIU HUI, Li L, *et al*. The combination of an oxygen-dependent degradation domain-regulated adenovirus expressing the chemokine RANTES/CCl5 and NK-92 cells exerts enhanced antitumor activity in hepatocellular carcinoma. *Oncol Rep* 2013;29:895–902.

21 DeHart CJ, Chahal JS, Flint SJ, *et al*. Extensive post-translational modification of active and inactivated forms of endogenous p53. *Mol Cell Proteomics* 2014;13:1–17.
22 Lewis MD, Roberts BJ. Role of the C-terminal α-helical domain of the von Hippel–Lindau protein in its E3 ubiquitin ligase activity. *Oncogene* 2004;23:2315–23.
23 Chang Y-W, Hung M-C, Su J-L, . The anti-tumor activity of E1A and its implications in cancer therapy. *Arch Immunol Ther Exp* 2014;62:195–204.
24 Fang L, Huang Y, Hu X, *et al*. A truncated minimal-E1a gene with potency to support adenoviral replication mediates antitumor activity by down-regulating neu expression and preserving Rb function. *Chem Biol Interact* 2009;181:1–7.
25 Georgi F, Greber UF. The adenovirus death protein – a small membrane protein controls cell lysis and disease. *FEBS Lett* 2020;594:1861–78.
26 Yotnda P, Zompeta C, Heslop HE, *et al*. Comparison of the efficiency of transduction of leukemic cells by fiber-modified adenoviruses. *Hum Gene Ther* 2004;15:1229–42.
27 Mato-Berciano A, Morgado S, Maliandi MV, *et al*. Oncolytic adenovirus with hyaluronidase activity that evades neutralizing antibodies: VCN-11. *Journal of Controlled Release* 2021;332:517–28.
28 Garris CS, Arlauckas SP, Kohler RH, *et al*. Successful anti-PD-1 cancer immunotherapy requires T Cell-Dendritic cell crosstalk involving the cytokines IFN-γ and IL-12. *Immunity* 2018;49:1148–61.
29 Dangaj D, Bruand M, Grimm AJ, *et al*. Cooperation between constitutive and inducible chemokines enables T cell engraftment and immune attack in solid tumors. *Cancer Cell* 2019;35:885–900.
30 Pol JG, Workenhe ST, Konda P, *et al*. Cytokines in oncolytic virotherapy. *Cytokine Growth Factor Rev* 2020;56:4–27.
31 Böttcher JP, Bonavita E, Chakravarty P, *et al*. Nk cells stimulate recruitment of cdc1 into the tumor microenvironment promoting cancer immune control. *Cell* 2018;172:e14:1022–37.
32 Bödder J, Zahan T, van Slooten R, *et al*. Harnessing the cDC1-NK cross-talk in the tumor microenvironment to battle cancer. *Front Immunol* 2021;11:631713.
33 Li F, Sheng Y, Hou W, *et al*. CCL5-armed oncolytic virus augments CCR5-engineered NK cell infiltration and antitumor efficiency. *J Immunother Cancer* 2020;8:e000131.